SIMULATING HIGHLY NONLINEAR SHIP-WAVE INTERACTION WITH EDGECFD

Thomas Miras[1]

Fernando A. Rochinha[1]

Renato N. Elias[1]

Alvaro L.G.A. Coutinho[1]

mirasthomas@nacad.ufrj.br

[1] High Performance Computing Center and Mechanical Engineering Department - Federal University of Rio de Janeiro (UFRJ)

Av. Horácio Macedo, 2030 - Centro de Tecnologia - Ilha do Fundão - Caixa Postal 68516, Rio de Janeiro, RJ - CEP 21941-598 - Brasil

José L.D. Alves[2]

Carlos E. Silva[2]

[2] Laboratory of Computational Methods in Engineering Civil Engineering Department - Federal University of Rio de Janeiro (UFRJ)

Av. Horácio Macedo, 2030 - Centro de Tecnologia - Ilha do Fundão - Caixa Postal 68516, Rio de Janeiro, RJ - CEP 21941-598 - Brasil

Abstract. *The coupling between a rigid body and an incompressible fluid is investigated. Within the framework of ALE, EdgeCFD uses edge-based parallel finite elements for the Navier Stokes equations and the VOF approach to describe the free surface evolution. Mesh updating is accomplished by a parallel edge-based solution of a non-homogeneous scalar diffusion problem in each spatial coordinate. We use here a staggered in time coupling and focus on the translational, rotation of the rigid body and the time integration scheme implementation. We compare the coupling approach with results coming from the literature and an industrial test case is studied considering a FPSO vessel interacting with waves.*

Keywords: *Fluid-structure-interaction, ALE, Rigid body motion, Time integration scheme*

1 INTRODUCTION

In the context of Fluid-Structure Interaction (FSI), offshore engineering presents a wide range of complex problems such as wave breaking on ships, green water on decks, the sloshing of liquids in tanks or highly nonlinear wave-body interaction. Those problems are of interest as consequences of the liquid movements can be dramatic. Thus, there exists a need to understand and estimate the interaction between the structure and the incompressible liquid with free surface. One can in particular cites the important works done in Fluid-Structure Interaction by Donea and Huerta (2003), Bazilevs et al. (2013) or Hughes (2012).

For FSI problems with a single fluid, moving mesh methods within the framework of the Arbitrary Lagrangian Eulerian (ALE) method, are often preferred when large body motions have to be taken into account. One does not give details about this method here, but we rather refer the interested reader to the literature that describes the method or addressing attention to a particular aspect of the overall methodology; Souli and Benson (2013); Bungartz and Schäfer (2006); Löhner (2008); Calderer and Masud (2010); Farhat et al. (2010).

One of the challenges here is to treat the free-surface problem. The different existing methods to describe the motion of the free surface can be classified as *interface tracking* or *interface capturing* methods. For interface tracking methods, a Lagrangian approach is considered and the grid is deformed and moves in order to follow the fluid flow. This approach is also suitable for meshless methods, one can cite the Smoothed Particle Hydrodynamics; Gomez-Gesteira et al. (2010), Particle Finite Element Methods; Larese et al. (2008) and Soroban grids; Takizawa et al. (2007) as examples of interface tracking methods. Interface capturing methods have emerged as a cost effective alternative to interface tracking methods. Eulerian in their concept, they rely on a unique and fixed computational grid to capture the interface evolution. The volume-of-fluid (VOF) method, firstly proposed in Hirt and Nichols (1981), and the level set method; Sethian (1999) are today the most important interface capturing techniques. The works of Elias and Coutinho (2007); Lins et al. (2010); Tezduyar et al. (1998) and Bruchon et al. (2009) are examples of unstructured grid formulations based on the finite element method to solve free-surface flows using these methods.

The problem is rather more difficult if we consider a structure interacting with two fluids. For Wall et al. (2007), a coupled partitioned approach for this problem is proposed. However, a simple model for the free-surface treatment is used and this somewhat limits its applicability. Nevertheless they underline that designing appropriate FSI schemes including free surface is not trivial. For Tanaka and Kashiyama (2006), an ALE finite element method for FSI problems with a free-surface using a mesh re-generation scheme is presented. Two-dimensional examples of falling objects in water show its effectiveness. VOF and Level Set methods associated to rigid body dynamics are applied to three dimensional FSI problems of ship hydrodynamics in Akkerman et al. (2012); Carrica et al. (2007); Formaggia et al. (2008). In Elias et al. (2009), the VOF parallel edge-based stabilized finite element solver Elias and Coutinho (2007) is extended to simulate three-dimensional wave-structure interaction problems induced by a piston-type wave maker. The piston movement is treated by ALE formulation, however, the formulation considered only mesh movements in one dimension. In the present work we extend the simulation capabilities of the solver including robust general mesh movement strategies and rigid body dynamics.

One focuses on the interaction between the rigid body and the fluid, and the time integration of the governing equations of the rigid body dynamics. The results presented are in the continuity of previous works Alves et al. (2012) where an implicit-explicit time integration scheme for the

rigid body motion was used. An Adams-Bashforth explicit scheme was used for the velocity or the rotational velocity and a Crank-Nicolson implicit scheme for the displacement or the angle of rotation. We extend the existing simulation capabilities focusing on the implementation of a time integration scheme adapted for both translational and rotational rigid body motion based an the implicit Newmark scheme. A Predictor/Corrector method is used to consider implicit time integrations for our staggered scheme. A particular attention is given for the non linear equation for rotations to take into account the non-commutative nature of a three dimensional rotation. In section 2, one will first focus on the theoretical part presenting the equations of the different physical phenomena involved in the problem: incompressible fluid flow, capturing method for the free surface position, mesh displacement and rigid body motion. One will particularly study the staggered time marching algorithm and the coupling setup (section 3 and 4).
These formulations are applied on different test cases in section 5 to both validate and show the capabilities of the coupling method. First, a vibrating plate in an incompressible liquid is considered. This test case is inspired from Hesch et al. (2014); Robertson et al. (2003); Li et al. (2000) that deal with Vortex Induced Vibration problems. It allows a comparison with different coupling methods and codes found in the literature. Finally, one applies the formulation on an industrial case, considering the interaction between a FPSO vessel and waves. The paper ends with a summary of our main conclusions.

2 EQUATIONS OF MOTION AND COUPLING

We consider here a staggered scheme where data exchange through boundary conditions allows the coupling between the equations (weak coupling). For a recent survey of multiphysics modeling and methods for coupling one can refer to Keyes et al. (2013).

2.1 Incompressible flow

The problem of interest concerns here the coupling between an incompressible Newtonian fluid and a rigid body, respectively governed by the Navier-Stokes equation and the Newton-Euler equations. The unknowns for the fluid are the velocity and the pressure $(\mathbf{u}, p)$, the displacement of the mass center $\mathbf{x}$ is considered for the structure. In the ALE frame of reference, defined over a space-time domain noted $\Omega \times [0, t_f]$, the Navier-Stokes equation of an incompressible Newtonian fluid is given by:

$$\begin{aligned} \rho_F \left(\frac{\partial \mathbf{u}}{\partial t} + (\mathbf{u} - \mathbf{u}_{mesh}) \cdot \nabla \mathbf{u} - \mathbf{b} \right) - \nabla \cdot \sigma = & \;\; 0 \\ \nabla \cdot \mathbf{u} = & \;\; 0 \end{aligned} \tag{1}$$

t is the time variable, $\mathbf{u}_{mesh}$ is the reference frame velocity, $\mathbf{b}$ is the body force vector, and ρ_F the fluid density. σ is the Cauchy stress tensor which is written for an incompressible Newtonian fluid:

$$\sigma(p, \mathbf{u}) = -p\mathbf{I} + \mu \left(\nabla \mathbf{u} + (\nabla \mathbf{u})^{\intercal} \right) \tag{2}$$

where $\mathbf{I}$ is the identity and μ the dynamic viscosity. In the present work, the classic Smagorinsky turbulence model is used where the viscosity μ is augmented by a subgrid-scale viscosity. The natural boundary conditions can be written as:

$$\begin{aligned} \mathbf{u} &= \mathbf{u}_E \quad \text{on } \Gamma_E \\ \mathbf{u} &= \dot{\mathbf{x}}_L \quad \text{on } \Gamma_L \\ \sigma \cdot \mathbf{n} &= \mathbf{h} \quad \text{on } \Gamma_h \end{aligned} \tag{3}$$

Γ_E is the Eulerian boundary, Γ_L is the Lagrangian boundary, i.e., the moving rigid body surface, and $\mathbf{h}$ is the applied traction force on Γ_h with $\mathbf{n}$ its outward normal vector. $\mathbf{u}_E$ and $\mathbf{x}_L$ are the fluid velocity on Γ_E and the Fluid-Structure interface displacement on Γ_L. One has $\partial\Omega = \Gamma_E \cup \Gamma_L \cup \Gamma_h$. One considers here two fluids (air and water) respectively occupying the domains Ω_A and Ω_B such that $\Omega = \Omega_A \cup \Omega_B$. Both domains are separated by a moving internal interface $\Gamma_{int}(t)$. The position of Γ_{int} is computed considering the following considerations (surface tensions between fluids are neglected):

$$\mathbf{u}_A = \mathbf{u}_B \quad \text{and} \quad \sigma_A \cdot \mathbf{n}_{int} = \sigma_B \cdot \mathbf{n}_{int} \tag{4}$$

$\mathbf{n}_{int}$ is the unit normal vector to the interface of Γ_{int}.

2.2 Interface capturing

In the volume-of-fluid method Hirt and Nichols (1981), a scalar marking function $\phi \in [0, 1]$ can be employed to capture the position of the interface between the fluid A ($\phi = 1$) and B ($\phi = 0$) by simply using the fluids fraction relationship. The function ϕ depends on fluid velocity $\mathbf{u}$ and is the solution of the transport equation written in the ALE framework:

$$\frac{\partial \phi}{\partial t} + \nabla \cdot ((\mathbf{u} - \mathbf{u}_{mesh})\, \phi) = 0 \quad \text{in}\Omega \tag{5}$$

The position of Γ_{int} is defined by the isovalue contour $\phi = \phi_C$ (usually $\phi_C = 0.5$) . Thus, the fluid density and viscosity are interpolated as follows:

$$\rho = \phi\rho_A + (1 - \phi)\,\rho_B \quad \mu = \phi\mu_A + (1 - \phi)\,\mu_B \tag{6}$$

2.3 Mesh movement

Among the different options available for addressing node repositioning, one considers here the scheme proposed in Masud and Hughes (1997) and extended for three dimensional application in Kanchi and Masud (2007); Masud et al. (2007). Nodes are repositioned as result of the solution of three scalar Boundary Value Problems:

$$\begin{aligned} \nabla \cdot ([1 + \tau_{mesh}]\, \nabla)\, x_N^i &= 0 \quad \text{with } i = 1, ..., n_{sd} \\ \mathbf{x}_N &= \mathbf{x}_L \quad \text{on } \Gamma_L \\ \mathbf{x}_N &= \mathbf{0} \quad \text{on } \partial\Omega \setminus \Gamma_L \end{aligned} \tag{7}$$

n_{sd} is the number of space dimensions, $\mathbf{x}_N$ is the vector of nodal displacements and τ_{mesh} is an artificial diffusivity computed for each element e of the mesh according to Eq. (8).

$$\tau_{mesh}(e) = \frac{1 - V_{min}/V_{max}}{V_e/V_{max}} \tag{8}$$

The mesh velocity is deduced from $\mathbf{x}_N$ and $\mathbf{u}_{mesh} = \mathbf{x}_N/\Delta t$. Δt being the time-step. V_{min}, V_{max} and V_e are respectively the least, the largest and the current volume in the mesh. τ_{mesh} has the crucial role of stiffening the elements in the immediate neighborhood of the body, allowing mesh distortion in the far field where large elements are usually located Masud et al. (2007); Kanchi and Masud (2007).

2.4 Rigid body motion

The rigid body motions are described by the 6 degrees of freedoms referred to its center of mass. Body weight and hydrodynamic forces acting of the rigid body's surface are summed-up as resulting forces. Let $\mathbf{f}$ be the hydrodynamic force on the body and $\mathbf{m}$ be the resulting moment acting on the rigid body mass center. The translational and rotational movements are given by the Newton-Euler equations:

$$m\mathbf{a} = \mathbf{f}_{tot} \tag{9}$$

$$\mathbf{J}\,\dot{\mathbf{\Omega}} + \mathbf{\Omega} \times \mathbf{J}\,\mathbf{\Omega} = \mathbf{m} \tag{10}$$

where Eq. (10) is expressed in the body frame. m is the mass of the body, $\mathbf{J}$ the tensor of inertia of the body referred to its mass center (computed with respect to a reference system attached to the body, $\mathbf{J}$ is constant), $\mathbf{a}$ is the acceleration of the body and $\mathbf{\Omega}$ is the angular velocity expressed in the body frame. $\mathbf{f}_{tot}$ is the total force applied on the rigid body and equals $\mathbf{f} + m\mathbf{g}$ ($\mathbf{g}$ representing the gravitational field). The hydrodynamic force $\mathbf{f}$ and the moment $\mathbf{m}$ applied on the immersed body and expressed in the body frame are computed according the following relations:

$$\mathbf{f} = \sum_{j=1}^{n_L} \mathbf{f}_j \qquad \mathbf{m} = \sum_{j=1}^{Ne} \mathbf{r}_j \wedge \mathbf{f}_j \tag{11}$$

where n_L is the number of nodes lying on the Lagrangian boundary (the rigid body surface), $\mathbf{f}_j$ represents the nodal forces applied on the body and computed from internal forces (see Alves et al. (2012)), and $\mathbf{r}_j$ are vectors between the center of mass of the rigid body and the application point of forces $\mathbf{f}_j$. In the rest, the index $n+i$, $i \in [\![-1;1]\!]$ corresponds to the time step $n+i$ ($t = t_{n+i}$).

3 TIME INTEGRATION SCHEMES

3.1 Translational movement

Generalized-α method, A well known and widely used scheme is the generalized-α method which was originally developed by Chung and Hulbert (1993). Four parameters, α_a, β, α, and γ are used and define the characteristics of the algorithm and the evolution of the displacement $\mathbf{x}^{n+1}$ and the velocity $\mathbf{v}^{n+1}$. For particular values of those parameters, one obtains classical time integration schemes such as the mid-point rule, Newmark method, HHT method, etc.

The equation of motion is expressed at an intermediate time level t^{α_a} between t^n and t^{n+1}, and the force at an intermediate time level t^{α} (see Table 1). $\mathbf{x}^{n+1}$ and $\mathbf{v}^{n+1}$ are given by the Newmark scheme, see Newmark (1959).

Table 1: Generalized-α time integration scheme for translations.

$$
\begin{aligned}
m\mathbf{a}^{\alpha_a} &= \mathbf{f}_{tot}^{\alpha} \\
\mathbf{x}^{n+1} &= \mathbf{x}^n + \Delta t \mathbf{v}^n + \Delta t^2 \left(\left(\tfrac{1}{2} - \beta\right)\mathbf{a}^n + \beta \mathbf{a}^{n+1}\right) \\
\mathbf{v}^{n+1} &= \mathbf{v}^n + \Delta t \left((1-\gamma)\mathbf{a}^n + \gamma \mathbf{a}^{n+1}\right)
\end{aligned}
$$

$$
\begin{aligned}
\mathbf{x}^{\alpha} &= (1-\alpha)\,\mathbf{x}^n + \alpha \mathbf{x}^{n+1} \\
\mathbf{v}^{\alpha} &= (1-\alpha)\,\mathbf{v}^n + \alpha \mathbf{v}^{n+1} \\
\mathbf{f}^{\alpha} &= (1-\alpha)\,\mathbf{f}^n + \alpha \mathbf{f}^{n+1} \\
\mathbf{a}^{\alpha_a} &= (1-\alpha_a)\,\mathbf{a}^n + \alpha_a \mathbf{a}^{n+1}
\end{aligned}
$$

3.2 Rotational movement

Among the numerous contributions on the topic, one has to cite the fundamental articles of Simo and Vu-Quoc (1988, 1986) who represented the rotations using the special orthogonal Lie group. Géradin and Cardona (1993) then extended those works to flexible multibody dynamics. We will first present the parametrization of the problem, the equation of rotation and the time integration scheme used. For more details concerning the demonstrations see Géradin and Rixen (1995); Säfström (2009).

Parametrization, To describe the mechanism of rotation we will consider two frames of reference, the spatial (or inertial) frame and the material (or body) frame, respectively given by sets of orthogonal base vectors. Let $\mathbf{B}_{space}$ and $\mathbf{B}_{body}$ be the base vector matrices. A particular attention has to be made concerning the definition of the rotation matrix $\mathbf{R}$. We introduce $\mathbf{R}$ such as $\mathbf{B}_{body} = \mathbf{R}\mathbf{B}_{space}$. The matrix $\mathbf{R}$ is then the change-of-basis matrix between $\mathbf{B}_{space}$ and $\mathbf{B}_{body}$. Therefor $\mathbf{R}$ belongs to the orthogonal group $SO(3)$ of dimension 3, defined by:

$$
SO(3) = \left\{\mathbf{R} \,:\, \mathbb{E}^3 \to \mathbb{E}^3 \text{ linear } \mathbf{R}^{\intercal}\mathbf{R} = \mathbf{I},\ \det(\mathbf{R}) = 1\right\} \tag{12}
$$

where $\mathbb{E}^3$ is the three-dimensional Euclidean space. The Euler's theorem states that for any rotation matrix, one can associate an angle and an axis of rotation. The orthonormal property of $\mathbf{R}$ can be translated into 6 constraints and implies that $\mathbf{R}$ can be expressed using three parameters. Among the different ways of writing the rotation matrix, one choses the Rodrigues formula. Let $\mathbf{\Psi}$ be the rotation vector associated to $\mathbf{R}$ such as $\mathbf{\Psi} = A\mathbf{n}_u$, $\mathbf{n}_u$ being a unit vector. $\widetilde{\mathbf{n}_u}$ is the skew-symmetric matrix associated to the vector $\mathbf{n}_u = [n_1\, n_2\, n_3]^{\intercal}$ such as, for an arbitrary vector $\mathbf{a}$:

$$
\widetilde{\mathbf{n}_u}\mathbf{a} = \mathbf{n}_u \times \mathbf{a} \quad \text{and} \quad \widetilde{\mathbf{n}_u} = \begin{bmatrix} 0 & -n_3 & n_2 \\ n_3 & 0 & -n_1 \\ -n_2 & n_1 & 0 \end{bmatrix} \tag{13}
$$

The exponential representation of $\mathbf{R}$ and $\mathbf{\Psi}$ is given by:

$$
\mathbf{R} = \exp \widetilde{\mathbf{\Psi}} = \mathbf{I} + \widetilde{\mathbf{\Psi}} + \frac{1}{2!}\widetilde{\mathbf{\Psi}}^2 + \frac{1}{3!}\widetilde{\mathbf{\Psi}}^3 + ... \tag{14}
$$

The Rodrigues formula gives a more convenient expression, see Géradin and Rixen (1995):

$$\mathbf{R} = \mathbf{I} + \frac{\sin \|\mathbf{\Psi}\|}{\|\mathbf{\Psi}\|}\widetilde{\mathbf{\Psi}} + \frac{1-\cos\|\mathbf{\Psi}\|}{\|\mathbf{\Psi}\|^2}\widetilde{\mathbf{\Psi}}\widetilde{\mathbf{\Psi}} \tag{15}$$

We consider now a rotation of the rigid body around a fixed point. Let P be a point on the body. The vector $\mathbf{x}^P$ designates the position of P and can be expressed in body or spatial coordinates. Let $\mathbf{X}^P$ be the vector corresponding to the position of P at the reference configuration: $\mathbf{x}^P = \mathbf{R}\mathbf{X}^P$. The velocity vector $\mathbf{v}^P$ is given by the time derivative of $\mathbf{x}^P$ and we have: $\mathbf{v}^P = \dot{\mathbf{R}}\mathbf{R}^\intercal\mathbf{x}^P$. One can show that the matrix $\dot{\mathbf{R}}\mathbf{R}^\intercal$ is skew symmetric writing the time derivative of $\mathbf{R}\mathbf{R}^\intercal$. Considering material coordinates we can also write: $\mathbf{V}^P = \mathbf{R}^\intercal\mathbf{v}^P = \mathbf{R}^\intercal\dot{\mathbf{R}}\mathbf{X}^P$. Thus, introducing the matrix of angular velocities $\widetilde{\mathbf{\Omega}}_S$ and $\widetilde{\mathbf{\Omega}}$ expressed respectively in spatial and material (body frame) coordinates, one has the following expressions:

$$\widetilde{\mathbf{\Omega}}_S = \dot{\mathbf{R}}\mathbf{R}^\intercal \quad \widetilde{\mathbf{\Omega}} = \mathbf{R}^\intercal\dot{\mathbf{R}} \quad \text{and} \quad \widetilde{\mathbf{\Omega}}_S = \dot{\mathbf{R}}\widetilde{\mathbf{\Omega}}\dot{\mathbf{R}}^\intercal \tag{16}$$

$\mathbf{\Omega}$ and $\mathbf{\Omega}_S$ can be expressed using $\mathbf{\Psi}$:

$$\mathbf{\Omega} = \mathbf{T}\dot{\mathbf{\Psi}} \quad \text{and} \quad \mathbf{\Omega}_S = \mathbf{T}^\intercal\dot{\mathbf{\Psi}} \tag{17}$$

and

$$\mathbf{T} = \mathbf{I} + \left(\frac{\cos\|\mathbf{\Psi}\|-1}{\|\mathbf{\Psi}\|^2}\right)\widetilde{\mathbf{\Psi}} + \left(1 - \frac{\sin\|\mathbf{\Psi}\|}{\|\mathbf{\Psi}\|}\right)\frac{\widetilde{\mathbf{\Psi}}\widetilde{\mathbf{\Psi}}}{\|\mathbf{\Psi}\|^2} \tag{18}$$

$\mathbf{T}$ being an operator defined in Géradin and Rixen (1995); Mäkinen (2001).

Compound rotation, The compound rotation is defined using the left translation map of $SO(3)$, $\mathbf{R}_{incr}$ being an incremental rotation matrix, we have:

$$\mathbf{R}_{new} = \mathbf{R}\mathbf{R}_{incr} = \mathbf{R}\exp(\widetilde{\mathbf{\Theta}}_{\mathbf{R}}) \tag{19}$$

where $\widetilde{\mathbf{\Theta}}_{\mathbf{R}}$ is the incremental rotation vector with respect to the base point $\mathbf{R}$ (in the rest, we will keep the notation $\widetilde{\mathbf{\Theta}}$). $\widetilde{\mathbf{\Theta}}$ corresponds to the material incremental rotation vector. Introducing the spatial incremental rotation vector $\widetilde{\theta}_S$, one has: $\theta_S = \mathbf{R}\mathbf{\Theta}$. Introducing the tangential vector spaces $T_{\mathbf{R}}SO(3)$ and $T_{\mathbf{I}}SO(3)$ with respect to the base points $\mathbf{R}_{old}$ and $\mathbf{I}$ on the rotation manifold $SO(3)$ defined by Eq. (12), $\widetilde{\mathbf{\Theta}}$ belongs to $T_{\mathbf{R}}SO(3)$, and $\widetilde{\mathbf{\Psi}}$ belongs to $T_{\mathbf{I}}SO(3)$. Then, it has to be noticed that the increment of the total material rotation tensor $\widetilde{\mathbf{\Psi}}$, written $\Delta\widetilde{\mathbf{\Psi}}$, is different from $\widetilde{\mathbf{\Theta}}$. Rewriting Eq. (19) with the exponential mapping one has:

$$\exp(\widetilde{\mathbf{\Psi}} + \Delta\widetilde{\mathbf{\Psi}}) = \exp\widetilde{\mathbf{\Psi}}\exp(\widetilde{\mathbf{\Theta}}) \neq \exp\widetilde{\mathbf{\Psi}}\exp(\Delta\widetilde{\mathbf{\Psi}}) \tag{20}$$

Indeed, $\Delta\widetilde{\mathbf{\Psi}}$ belong to different vector spaces: $\Delta\widetilde{\mathbf{\Psi}} \in T_{\mathbf{I}}SO(3)$ and the linear mapping between $T_{\mathbf{R}}SO(3)$ and $T_{\mathbf{I}}SO(3)$ is given by the operator $\mathbf{T}$ in Eq. (18), see Simo and Vu-Quoc (1988). The relation between the vectors $\Delta\mathbf{\Psi}$ and $\mathbf{\Theta}$ is given by: $\mathbf{\Theta} = \mathbf{T}\Delta\mathbf{\Psi}$.

Equation of motion, The equation of rotation can be expressed considering the angular moment of the system. By definition, the angular moment in the spatial frame is given by:

$$\mathbf{h}_S = \mathbf{I}_S\mathbf{\Omega}_S \tag{21}$$

where $\mathbf{I}_S$ is the inertial tensor in the spatial frame. Let $\mathbf{h}$ be the angular moment in the body frame such as $\mathbf{h} = \mathbf{J}\boldsymbol{\Omega} = \mathbf{R}^{\intercal}\mathbf{h}_S$. Making an appropriate choice for the rigid body frame, the matrix $\mathbf{J}$ can be diagonal. The law of conservation of angular moment states that the time derivative of $\mathbf{h}_S$ equals the external moment $\mathbf{M}$ applied on the system:

$$\dot{\mathbf{R}}\mathbf{J}\boldsymbol{\Omega} + \mathbf{R}\mathbf{J}\dot{\boldsymbol{\Omega}} = \mathbf{M} \tag{22}$$

Using Eq. (16) and introducing the moment in the body frame $\mathbf{m} = \mathbf{R}^{\intercal}\mathbf{M}$ one finds Eq. (10) which can also be demonstrated via a variational principle as suggested by Géradin and Rixen (1995) or the Noether's theorem used by Säfström (2009):

$$\mathbf{J}\,\dot{\boldsymbol{\Omega}} + \widetilde{\boldsymbol{\Omega}}\mathbf{J}\,\boldsymbol{\Omega} = \mathbf{m} \tag{23}$$

Only variables expressed in the body frame are considered.

Time integration scheme, The results obtained in section 3.2 are now generalized considering a discretization in time. The problem of time stepping update can be formulated as follows: Given a configuration at time step n: $\mathbf{R}^n$, $\boldsymbol{\Omega}^n$, and $\mathbf{A}^n$, find the updated configuration $\mathbf{R}^{n+1}$, $\boldsymbol{\Omega}^{n+1}$, and $\mathbf{A}^{n+1}$. One rewrites Eq. (19):

$$\mathbf{R}^{n+1} = \mathbf{R}^n \exp(\widetilde{\boldsymbol{\Theta}}^n) \tag{24}$$

Simo and Vu-Quoc (1988) propose an extension of the Newmark formulas to the orthogonal group $SO(3)$. The equation of rotation is non linear and one can solve it using the classical Newton method writing the iterative form of the Newmark time integration scheme for rotations. Simo and Vu-Quoc (1988) and Cardona and Géradin (1988) give the modified Newmark scheme starting with the expression of $\boldsymbol{\Theta}^n_{(i+1)}$ and $\boldsymbol{\Theta}^n_{(i)}$. The subscript i identifies the intermediate step between n and $n+1$. The iterative variables are given in Table 2. Mäkinen (2001) gives a critical

Table 2: Iterative variables

$\boldsymbol{\Theta}^n_{(i+1)}$	=	$\boldsymbol{\Theta}^n_{(i)} + \Delta\boldsymbol{\Theta}^n_{(i)}$
$\mathbf{R}^{n+1}_{(i+1)}$	=	$\mathbf{R}^{n+1}_{(i)} \exp(\Delta\widetilde{\boldsymbol{\Theta}}^n_{(i)})$
$\exp(\widetilde{\boldsymbol{\Theta}}^n_{(i+1)})$	=	$\exp(\widetilde{\boldsymbol{\Theta}}^n_{(i)}) \exp(\Delta\widetilde{\boldsymbol{\Theta}}^n_{(i)})$
$\boldsymbol{\Omega}^{n+1}_{(i+1)}$	=	$\boldsymbol{\Omega}^{n+1}_{(i)} + \frac{\gamma}{\Delta t\beta}\Delta\boldsymbol{\Theta}^n_{(i)}$
$\mathbf{A}^{n+1}_{(i+1)}$	=	$\mathbf{A}^{n+1}_{(i)} + \frac{1}{\Delta t^2\beta}\Delta\boldsymbol{\Theta}^n_{(i)}$

study of this scheme on the manifold of finite rotations. Indeed, it is underlined that $\boldsymbol{\Omega}^n$ and $\mathbf{A}^n$ belong to a different tangent space than $\boldsymbol{\Omega}^{n+1}$ and $\mathbf{A}^{n+1}$ we call respectively those tangent spaces $T_{\mathbf{R}^n}$ and $T_{\mathbf{R}^{n+1}}$. This problem also occurs in Table 2 where $\Delta\boldsymbol{\Theta}^n \in T_{\mathbf{R}^n}$. The rotation matrix $\mathbf{R}$ depends on time and the base point $\mathbf{R}$ on the rotation manifold moves between two instants. Usually, the Newmark scheme or its iterative form in Table 2 are used in the literature but it has to be specified that these are approximated.
In order to avoid this problem, one can use the operator $\mathbf{T}$ introduced with Eq. (18). Applying the Newmark scheme on $\boldsymbol{\Theta}^n$ and $\dot{\boldsymbol{\Theta}}^n$ as suggested by Cardona and Géradin (1988). This leads to

Table 3: Corrected Iterative Newmark Method

$$\begin{aligned}
\mathbf{\Theta}^n_{(i+1)} &= \mathbf{\Theta}^n_{(i)} + \Delta\mathbf{\Theta}^n_{(i)} \\
\mathbf{\Omega}^{n+1}_{(i+1)} &= \mathbf{\Omega}^{n+1}_{(i)} + \tfrac{\gamma}{\Delta t \beta}\mathbf{T}_n \Delta\mathbf{\Theta}^n_{(i)} \\
\mathbf{A}^{n+1}_{(i+1)} &= \mathbf{A}^{n+1}_{(i)} + \tfrac{1}{(\Delta t)^2 \beta}\mathbf{T}_n \Delta\mathbf{\Theta}^n_{(i)} + \tfrac{\gamma}{\Delta t \beta}\dot{\mathbf{T}}_n \Delta\mathbf{\Theta}^n_{(i)}
\end{aligned}$$

the corrected iterative Newmark scheme presented in Table 3. $\mathbf{T}_n = \mathbf{T}(\mathbf{\Theta}^n_{(i)})$ is a map from $T_{\mathbf{R}^n}$ to $T_{\mathbf{R}^{n+1}}$. Thus, the vectors belong to the same vector space on the manifold for every iteration step (i). For the converged solution $\mathbf{\Theta}^n_{(m)}$ one has $\mathbf{R}^{n+1} = \mathbf{R}^n \exp(\widetilde{\mathbf{\Theta}}^n_{(m)})$. Mäkinen (2001) gives a comparative study between the approximative Newmark scheme and the corrected one using $\mathbf{T}$. For small incremental angles, the two schemes are equivalent and it is underlined that: "the justification of the modified Newmark-scheme arises rather from theoretical aspects than numerical accuracy". Nevertheless, the approach presented to obtain Table 3 becomes necessary when Reduced Order Models are used. One will thus just consider the iterative variables given by Table 2.

Due to its properties of stability, also presented for the translational movement, the mid-point scheme is prefered. Simo and Wong (1991) show that for incremental force free motion, this scheme exactly conserves the energy.

The discrete conservation law can be written as:

$$\mathbf{R}^{n+1}\mathbf{J}\mathbf{\Omega}^{n+1} - \mathbf{R}^n\mathbf{J}\mathbf{\Omega}^n - \Delta t \mathbf{M}^{n+1/2} = \mathbf{G}(\mathbf{\Theta}^n) = 0 \tag{25}$$

To solve this non linear equation by the Newton's method, one has to linearize $\mathbf{G}(\mathbf{\Theta}^n)$ around an intermediate step i and in the direction $\Delta\mathbf{\Theta}^n_{(i)} = \mathbf{\Theta}^n_{(i+1)} - \mathbf{\Theta}^n_{(i)}$ (see Table 2):

$$L_i\left(\mathbf{G}(\mathbf{\Theta}^n)\right) = \mathbf{G}(\mathbf{\Theta}^n_{(i)}) + \delta_i\left[\mathbf{G}(\mathbf{\Theta}^n_{(i)})\right](\Delta\mathbf{\Theta}^n_{(i)}) \tag{26}$$

where $\delta_i\,[.]$ is the directional derivative of $(.)$ in the direction $\Delta\mathbf{\Theta}^n_{(i)}$. With $\mathbf{K}^{n+1}_{(i)}$ and $\mathbf{Re}_{(i)}$ the tangent matrix and the residual are expressed as:

$$\mathbf{K}^{n+1}_{(i)}\Delta\mathbf{\Theta}^n_{(i)} = \mathbf{Re}_{(i)} = -\mathbf{G}(\mathbf{\Theta}^n_{(i)}) \quad \text{with } \mathbf{K}^{n+1}_{(i)} = \mathbf{R}^{n+1}_{(i)}\left[\frac{\gamma}{\Delta t \beta}\mathbf{J}\mathbf{T}_n - \widetilde{\mathbf{J}\mathbf{\Omega}_{(i)}}^{n+1}\right] \tag{27}$$

For more details about the algorithm, see Simo and Vu-Quoc (1988).

4 COUPLING SET UP

One has here a weakly coupled strategy (or staggered schemes) and the algorithm used in EdgeCFD does not provide the force at time step $n+1$ as the body equation is solved first. As reminded by Akkerman et al. (2012), a limit of staggered schemes is the time step that has to stay small. On the other hand, they have a shorter computational time than strongly coupled schemes and also allow the use of sub-solver softwares such as the VOF method. Dettmer and Perić (2012) also underline the fact that in the case of an incompressible fluid-structure interaction staggered schemes proposed in literature are not suitable and propose a staggered scheme using a predictor-corrector approach giving good results, with a wide range of applicability including problems with added mass effects. The Force/Moment applied on the Fluid-Structure interface is first predicted:

$$\begin{pmatrix} \mathbf{f}^{n+1} \\ \mathbf{m}^{n+1} \end{pmatrix} \approx \begin{pmatrix} \hat{\mathbf{f}}^{n+1} \\ \hat{\mathbf{m}}^{n+1} \end{pmatrix} = (1+\tau) \begin{pmatrix} \mathbf{f}^{n} \\ \mathbf{m}^{n} \end{pmatrix} - \tau \begin{pmatrix} \mathbf{f}^{n-1} \\ \mathbf{m}^{n-1} \end{pmatrix} \tag{28}$$

where $(\hat{\mathbf{f}}^{n+1}, \hat{\mathbf{m}}^{n+1})$ are the predicted Force / Moment. For $\tau = 1$ and a fixed time step one has a first order Newton-Gregory backward polynomials and for $\tau = 0$ the backward Euler method, see Cellier and Kofman (2006). If $\tau = 0$ the impact of the fluid on the solid is ignored. In Li et al. (2000), the author considers $\tau = \frac{1}{2}$ in his problem. Using the notation $(\mathbf{f}_*^{n+1}, \mathbf{m}_*^{n+1})$ for the Force / Moment computed after solving the incompressible fluid flow given by Eq. (1) (once $\mathbf{x}^{n+1}$ and $\mathbf{\Theta}^n$ are known), the corrected Force / Moment $(\mathbf{f}_C^{n+1}, \mathbf{m}_C^{n+1})$ are given as:

$$\begin{pmatrix} \mathbf{f}^{n+1} \\ \mathbf{m}^{n+1} \end{pmatrix} = \tau_C \begin{pmatrix} \mathbf{f}_*^{n+1} \\ \mathbf{m}_*^{n+1} \end{pmatrix} + (1-\tau_C) \begin{pmatrix} \hat{\mathbf{f}}^{n+1} \\ \hat{\mathbf{m}}^{n+1} \end{pmatrix} \tag{29}$$

the parameter τ_C has to be set and a natural choice is $\tau_C = 1/2$. If $\tau_C = 0$ the impact of the fluid on the solid is ignored. Small values of τ_C reduces the impact of added mass effect and allows to achieve unconditional stability, see Dettmer and Perić (2012). For every time step, the approach for coupling the different equations involved can be summed up as follow:

Given $(\mathbf{u}, \mathbf{u}_{mesh}, p, \phi)_{t=t_n}$ and $(\mathbf{x}, \mathbf{R})_{t=t_n}$

1. Compute nodal forces and resulting forces/moments $(\mathbf{f}_*^{n+1}, \mathbf{m}_*^{n+1})$ (see Eq. (11))
2. Compute $(\hat{\mathbf{f}}^{n+1}, \hat{\mathbf{m}}^{n+1})$ using Eq. (28)
3. Compute the rigid body motion $(\mathbf{x}, \mathbf{R})_{t=t_{n+1}}$ solving Eq. (9) and Eq. (10).
4. Compute mesh Displacement / instantaneous Velocity $\mathbf{u}_{mesh}^{n+1}$ solving the Boundary Value Problem in Eq. (7) and the updated position of the interface Γ_L
5. Solve the Navier Stokes equation in the ALE framework (see Eq. (1)) to obtain $(\mathbf{u}, p)_{t=t_{n+1}}$
6. Deduce $(\mathbf{f}_*^{n+1}, \mathbf{m}_*^{n+1})$ and $(\mathbf{f}^{n+1}, \mathbf{m}^{n+1})$ using Eq. (29)
7. Solve the VOF in Eq. (5) and update the free surface position

End of the loop: $n \leftarrow (n+1)$

The flow solver includes a Streamline-Upwind / Petrov-Galerkin (SUPG) and Pressure-Stabilizing / Petrov-Galerkin (PSPG) stabilized finite element formulation; an Implicit time marching scheme and advanced inexact nodal block-diagonal preconditioned Newton-Krylov solvers; Edge-based data structures to save memory and improve performance; support to message passing and hybrid parallel programming models (for more details concerning the flow solver see Elias et al. (2009); Elias and Coutinho (2007); Lins et al. (2010)). The advection equation given by Eq. (5) is solved by a fully implicit parallel edge-based SUPG finite element formulation. The algebraic system of equations resulting from the mesh movement BVP is solved by an edge-based conjugate gradient method with diagonal preconditioning.

5 TEST CASES

5.1 Rotating plate and Vortex Induced Vibration

A simple test case is first studied, allowing to evaluate the performances of the method in term of accuracy and robustness. A rigid plate is placed under an incompressible fluid flow. This test case was widely used, especially to study the rotational and translational galloping instabilities or vortex induced vibration (VIV). Those instabilities may occur when the vortex shedding frequency is close the natural frequency. One focuses on the rotational movement, translational movements are blocked and the plate can only rotates around its center of mass and according to one axis ($\mathbf{y}$) perpendicular to the plane of study, the setup is presented in Fig. 1. Robertson et al. (2003) and Li et al. (2000) consider a weak coupling using the ALE framework. Hesch et al. (2014); Yang and Stern (2012); Dettmer and Perić (2006) propose a strong coupling approach using respectively a mortar method, a simplified embedded-boundary formulation and a Newton-Raphson method. Only the 2D problem is presented in the literature and EdgeCFD is a 3D solver. One creates a 3D geometry with a depth equal to one in order to compare with existing results. The test case setup is given by Fig. 1. The *inlet* boundary condition is given by the normal velocity $U = \mathbf{u} \cdot \mathbf{n}$ of the fluid ($\mathbf{n}$ is the unit normal vector at the fluid boundary). The boundary condition *BC1* on the upper and bottom part of the fluid domain corresponds to $\mathbf{u} \cdot \mathbf{n} = 0$, and one has $p = 0$ for *BC2*. The non slip boundary condition is applied on the solid. To characterize the numerical experiments one introduces the mass

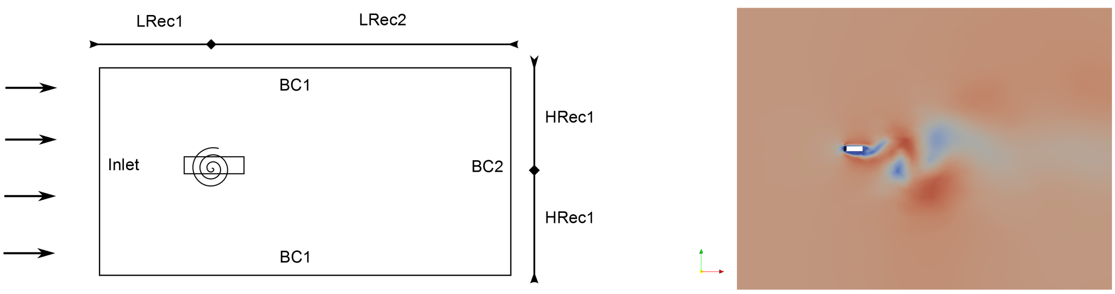

Figure 1: Scheme of the $2D$ problem. In meters, $Lrec1 = 25$ $Lrec2 = 55$, $Hrec1 = 30$. The length L of the plate is 4, the thickness h is 1. On the right an example of the flow around the plate at $t = 45(s)$ colored by the velocity magnitude with $n = 400$, $U_n = 40$, $Re = 250$, $k = 78.54$, $\xi = 0.25$.

moment of inertia ratio $n = I/(\rho h^4)$ where I, ρ and h are the moment of inertia according to the axis $\mathbf{y}$, the fluid density and h is the thickness of the plate. Δ is the ratio between the length of the plate and h. One also defines the reduced velocity $U_n = U/(f_n h)$. f_n is the natural frequency of the system such as $f_n = \frac{1}{2\pi}\sqrt{k/I}$ where k is the torsional stiffness constant. ξ is the damping ratio and Re the Reynolds number. Δt is the time step and Δx the space between nodes on the rigid body.

The Fig. 2 illustrate a typical result with an oscillation after a transient phase. The ratio between the natural frequency and the oscillation frequency f_o of the plate is $f_o/f_n = 0.7632$. The amplitude of the oscillation is around 0.2 (rad). As Hesch et al. (2014) underline, the common results found in the literature are within the interval $[0.76, 0.78]$ with an amplitude between 0.23 to 0.26 (rad). For this simulation $\Delta x = 0.08$ which is less than what is usually used (between 0.033 and 0.067). However, because of the weak coupling the time step has to stay small:

$\Delta t = 10^{-3}$ as it is done by Robertson et al. (2003). The simulation is in good agreement with the results found in the literature.
In Fig. 3, one shows for a different geometry and parameters, the oscillations of a square. With

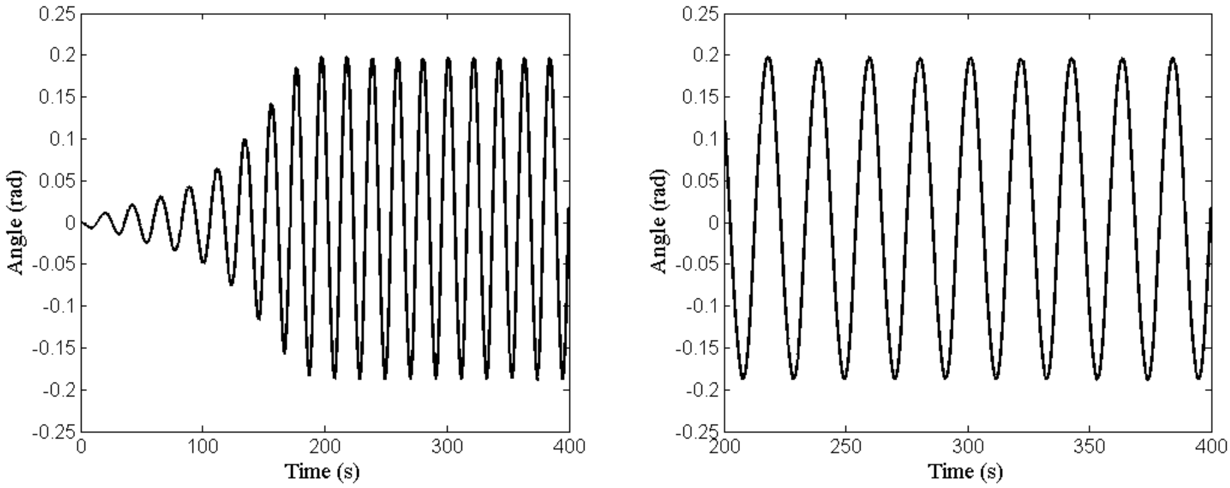

Figure 2: Representation of the angle of the plate (in radians) as a function of the time. $\Delta t = 10^{-3}$, $Re = 250$, $\xi = 0.25$, $n = 400$, $f_n = 0.0625$, $\Delta = 4$.

this particular shape, as it is noticed by Robertson et al. (2003) one expects a low amplitude for the galloping motion. This type of simulation illustrate the complex phenomenon of VIV. Two frequencies are observed, the first one is due to vortex shedding and the second one (lower) to the galloping motion.

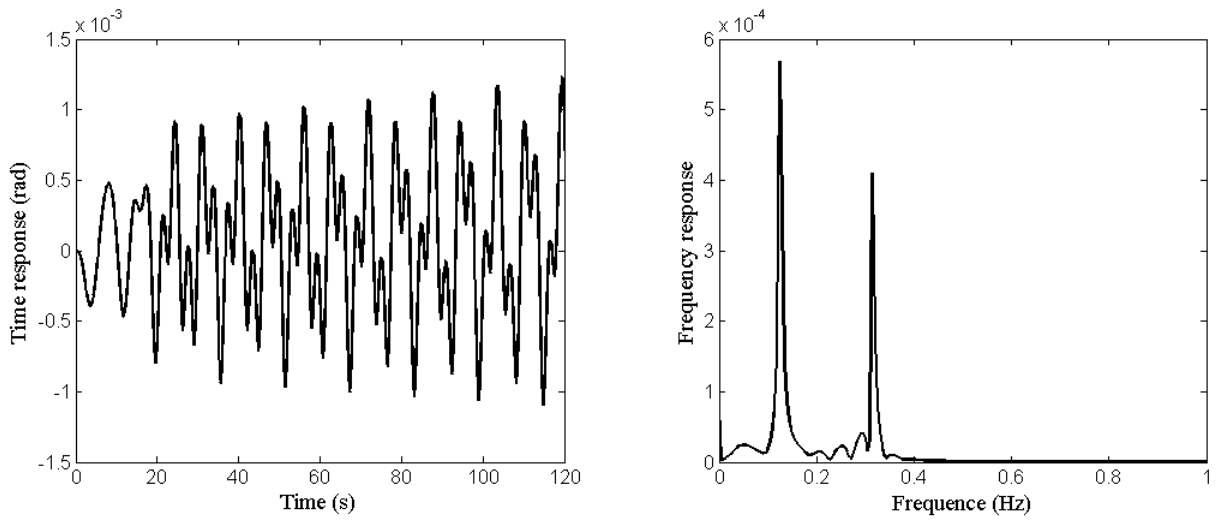

Figure 3: Oscillations of the plate for $\Delta = 1, , \xi = 0, n = 100, f_n = 0.0625$.

5.2 Wave-Ship Interaction

We consider now a more complex industrial test case were a FPSO vessel interacts with waves. Snapshots of the simulation is presented in Fig. 4. The ship axis is perpendicular to the waves that are created using the orbital velocity method, see Sleath (1984). On the boundary of the free surface domain wave absorbers are considered.

Figure 4: Representation of the system at time $t = 0$ s, $t = 1$ s,$t = 9$ s. The time step for this simulation is 10^{-3} seconds.

The ship is allowed to move according with the three degrees of freedom of rotation and the vertical direction. Fig. 5 gives the angular time response. From $t = 8$ seconds the ship is changing its direction starting a large rotation according to the vertical axis. The simulation stops due to the mesh distortion after a rotation of around $\pi/2$. The same simulation is made blocking the rotation around the vertical axis (the ship keep the same direction).

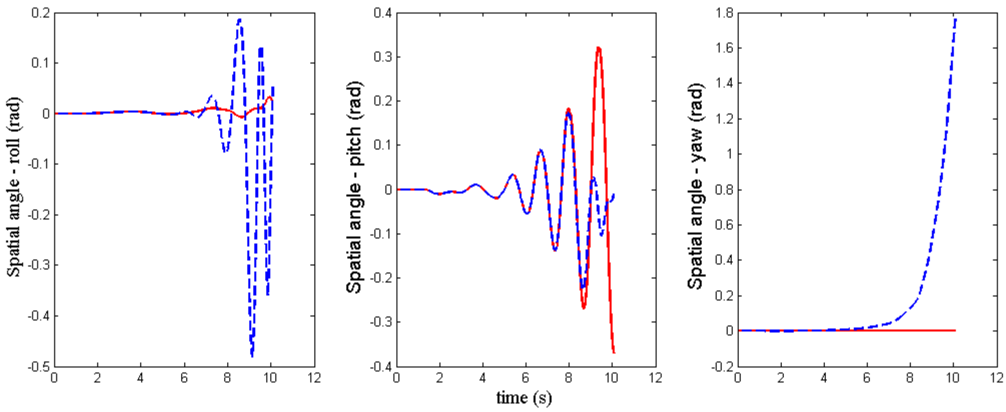

Figure 5: Angular time response of the FPSO vessel according to the three axis of rotation (from left to right: the roll, the pitch and the yaw). Dashed line: all rotations are allowed. Plain line: same conditions but the yaw movement is blocked.

6 CONCLUSION

The theoretical background for the coupling between a rigid body and a structure has been presented. A staggered scheme is used here and one considers a predictor / corrector approach. The translational and rotational equation of the rigid body motion have been investigated. The method proposed by Simo and Wong (1991) and implemented to solve the rotational movement of the rigid body is unconditionally stable, preserves energy and momentum. This method is applied on test cases with a 3D incompressible fluid flow considering or not a free surface. This complex configuration is treated within the ALE framework and using the home made software EdgeCFD. This system uses edge-based parallel finite elements for the Navier Stokes equations and the VOF approach to describe the free surface evolution. Mesh updating is accomplished by a parallel edge-based solution of a non-homogeneous scalar diffusion problem in each spatial

coordinate.
Focusing on the FSI part of the problem and especially the rotational movement, we present different test cases. The first one is widely used in the literature and allow to validate the accuracy and robustness of the code. Indeed, large deformation can be considered as shown by the second test case: a FPSO vessel interacting with waves.
In the future, one can imagine other test cases to continue the validation of the coupling set up. Sanders et al. (2011) study the problem buoyant bodies, presenting both analytical and experimental results.

REFERENCES

Akkerman, I., Bazilevs, Y., Benson, D., Farthing, M., and Kees, C. (2012). Free-surface flow and fluid-object interaction modeling with emphasis on ship hydrodynamics. *Journal of Applied Mechanics*, 79(1):010905.

Alves, J. L., Silva, C. E., Guevara, N. O., Coutinho, A. L., Elias, R. N., Rochinha, F. F., Martins, M. A., Ferreira, M. D., and Silva, D. F. (June 10-15 2012). Edgecfd-ale: A stabilized finite element system for fluid-structure interaction in offshore engineering. In *Proceedings of the ASME* 2012 31*st International Conference on Ocean, Offshore and Artic Engineering*.

Bazilevs, Y., Takizawa, K., and Tezduyar, T. E. (2013). *Computational Fluid-Structure Interaction Methods and Applications*. Wiley-Blackwell.

Bruchon, J., Digonnet, H., and Coupez, T. (2009). Using a signed distance function for the simulation of metal forming processes: Formulation of the contact condition and mesh adaptation. from a lagrangian approach to an eulerian approach. *International journal for numerical methods in engineering*, 78(8):980–1008.

Bungartz, H.-J. and Schäfer, M. (2006). *Fluid-structure interaction: modelling, simulation, optimisation*, volume 1. Springer Science & Business Media.

Calderer, R. and Masud, A. (2010). A multiscale stabilized ale formulation for incompressible flows with moving boundaries. *Computational Mechanics*, 46(1):185–197.

Cardona, A. and Géradin, M. (1988). A beam finite element non-linear theory with finite rotations. *Int. J. Numer. Methods Engrg*, 26:2403–2438.

Carrica, P. M., Wilson, R. V., Noack, R. W., and Stern, F. (2007). Ship motions using single-phase level set with dynamic overset grids. *Computers & Fluids*, 36(9):1415–1433.

Cellier, F. E. and Kofman, E. (2006). *Continuous system simulation*. Springer Science & Business Media.

Chung, J. and Hulbert, G. (1993). A time integration algorithm for structural dynamics with improved numerical dissipation: the generalized-α method. *Journal of Applied Mechanics*, 60:371–375.

Dettmer, W. and Perić, D. (2006). A computational framework for fluid-rigid body interaction: Finite element formulation and applications. *Computer Methods in Applied Mechanics and Engineering.*, 195:1633–1666.

Dettmer, W. G. and Perić, D. (2012). A new staggered scheme for fluid-structure interaction. *Internal journal for numerical methods in engineering*.

Donea, J. and Huerta, A. (2003). *Finite Element Methods for Flow Problems*. Wiley.

Elias, R., A.Gonçalves, M., Coutinho, A. L. G. A., Esperança, P., Martins, M., and M.Ferreira (2009). Free-surface flow simulation using stabilized edge-based finite element methods. In *In Proceeedings of ASME 2009 28th International Conference on Offshore Mechanics and Arctic Engineering OMAE, ASME.*

Elias, R. N. and Coutinho, A. L. G. A. (2007). Stabilized edge-based finite element simulation of free-surface flows. *International Journal for Numerical Methods in Fluids*, 54:965–993.

Farhat, C., Rallu, A., Wang, K., and Belytschko, T. (2010). Robust and provably second-order explicit–explicit and implicit–explicit staggered time-integrators for highly non-linear compressible fluid–structure interaction problems. *International Journal for Numerical Methods in Engineering*, 84(1):73–107.

Formaggia, L., Miglio, E., Mola, A., and Parolini, N. (2008). Fluid-structure interaction problems in free surface flows: Application to boat dynamics. *International Journal for Numerical Methods in Fluids*, 56:965–978.

Géradin, M. and Cardona, A. (1993). Finite element modeling concepts in multibody dynamics. In *Computer aided analysis of rigid and flexible mechanical systems*.

Géradin, M. and Rixen, D. (1995). Parametrization of finite rotations in computational dynamics: a review. *Revue européenne des éléments finis*, 4:497–553.

Gomez-Gesteira, M., Rogers, B. D., Dalrymple, R. A., and Crespo, A. J. (2010). State-of-the-art of classical sph for free-surface flows. *Journal of Hydraulic Research*, 48(S1):6–27.

Hesch, C., Gil, A., no, A. A. C., Bonnet, J., and Betsch, J. (2014). A mortar approach for fluid-structure interaction problems: Immersed strategies for deformable and rigid bodies. *Comput. Methods Appl. Mech. Engrg*, 278:853–882.

Hirt, C. W. and Nichols, B. D. (1981). Volume of fluid (vof) method for the dynamics of free boundaries. *Journal of computational physics*, 39(1):201–225.

Hughes, T. J. (2012). *The finite element method: linear static and dynamic finite element analysis*. Courier Dover Publications.

Kanchi, H. and Masud, A. (2007). A 3d adaptive mesh moving scheme. *International Journal for Numerical Methods in Fluids*, 54(6-8):923–944.

Keyes, D. E., Mcinnes, L. C., Woodward, C., Gropp, W., Myra, E., Pernice, M., Bell, J., Brown, J., Clo, A., Connors, J., Constantinescu, E., Estep, D., Evans, K., Farhat, C., Hakim, A., Hammond, G., Hansen, G., Hill, J., Isaac, T., Jiao, X., Jordan, K., Kaushik, D., Kaxiras, E., Koniges, A., Lee, K., Lott, A., Lu, Q., Magerlein, J., Maxwell, R., Mccourt, M., Mehl, M., Pawlowski, R., Randles, A. P., Reynolds, D., Rivière, B., Rüde, U., Scheibe, T., Shadid, J., Sheehan, B., Shephard, M., Siegel, A., Smith, B., Tang, X., Wilson, C., and Wohlmuth, B. (2013). Multiphysics simulations: Challenges and opportunities. *Int. J. High Perform. Comput. Appl.*, 27(1):4–83.

Larese, A., Rossi, R., Oñate, E., and Idelsohn, S. (2008). Validation of the particle finite element method (pfem) for simulation of free surface flows. *Engineering Computations*, 25(4):385–425.

Li, L., Sherwin, S., and Bearman, P. (2000). A moving frame of reference algorithm for fluid/structure interaction of rotating and translating bodies. *International journal for numerical methods in fluids*, pages 1–20.

Lins, E., Elias, R., Rochinha, F., and Coutinho, A. (2010). Residual-based variational multiscale simulation of free surface flows. *Computational Mechanics*, 46:545–557.

Löhner, R. (2008). *Applied computational fluid dynamics techniques: an introduction based on finite element methods*. John Wiley & Sons.

Mäkinen, J. (2001). Critical study of newmark-scheme on manifold of finite rotations. *Computer methods in applied mechanics and engineering*, 191:817–828.

Masud, A., Bhanabhagvanwala, M., and Khurram, R. A. (2007). An adaptive mesh rezoning scheme for moving boundary flows and fluid–structure interaction. *Computers & fluids*, 36(1):77–91.

Masud, A. and Hughes, T. J. (1997). A space-time galerkin/least-squares finite element formulation of the navier-stokes equations for moving domain problems. *Computer Methods in Applied Mechanics and Engineering*, 146(1):91–126.

Newmark, N. (1959). A method of computation for structural dynamics. *ASCE Journal of Engineering Mechanics Division*, 85.

Robertson, I., Li, L., Sherwin, S., and Bearman, P. (2003). A numerical study of rotational and transverse galloping rectangular bodies. *Journal of Fluids and Structures*, 17:681–699.

Säfström, N. (2009). *Modeling and simulation of rigid body and rod dynamics via geometric methods*. PhD thesis, NTNU.

Sanders, J., Dolbow, J. E., Mucha, P. J., and Laursen, T. A. (2011). A new method for simulating rigid body motion in incompressible two-phase flow. *International Journal for Numerical Methods in Fluids*, 67(6):713–732.

Sethian, J. A. (1999). *Level set methods and fast marching methods: evolving interfaces in computational geometry, fluid mechanics, computer vision, and materials science*, volume 3. Cambridge university press.

Simo, J. and Vu-Quoc, L. (1986). A three-dimensional finite-stain rod model, part 2: Computational aspects. *Computer methods in applied mechanics and engineering*, 58:79–116.

Simo, J. and Vu-Quoc, L. (1988). On the dynamics in space of rods undergoing large motions - a geometrically exact approach. *Computer methods in applied mechanics and engineering*, 66:125–161.

Simo, J. and Wong, K. K. (1991). Unconditionally stable algorithms for rigid body dynamics that exactly preserve energy and momentum. *International journal for numerical methods in engineering*, 31:19–52.

Sleath, J. (1984). *Sea bed mechanics*. Wiley, New York.

Souli, M. and Benson, D. J. (2013). *Arbitrary Lagrangian Eulerian and Fluid-Structure Interaction: Numerical Simulation*. John Wiley & Sons.

Takizawa, K., Yabe, T., Tsugawa, Y., Tezduyar, T. E., and Mizoe, H. (2007). Computation of free-surface flows and fluid–object interactions with the cip method based on adaptive meshless soroban grids. *Computational Mechanics*, 40(1):167–183.

Tanaka, S. and Kashiyama, K. (2006). Ale finite element method for fsi problems with free surface using mesh re-generation method based on background mesh. *International Journal of Computational Fluid Dynamics*, 20(3-4):229–236.

Tezduyar, T., Aliabadi, S., and Behr, M. (1998). Enhanced-discretization interface-capturing technique (edict) for computation of unsteady flows with interfaces. *Computer Methods in Applied Mechanics and Engineering*, 155(3):235–248.

Wall, W. A., Genkinger, S., and Ramm, E. (2007). A strong coupling partitioned approach for fluid–structure interaction with free surfaces. *Computers & Fluids*, 36(1):169–183.

Yang, J. and Stern, F. (2012). A simple and efficient direct forcing immerse boundary framework for fluid-structure interactions.